scientific reports

Check for updates

OPEN

Construction and validation of a novel model for guiding targeted combined immunotherapy in advanced hepatocellular carcinoma

Haibin Tu[1], Siyi Feng[1], Lihong Chen[1], Yujie Huang[1], Juzhen Zhang[1], Suyu Peng[1], Dingluan Lin[2] & Xiaojian Ye[3,4]✉

In addressing the challenge of optimizing targeted combined immunotherapy for advanced hepatocellular carcinoma (HCC), this study developed and validated a novel prognostic model, the Target Immunotherapy Predict Model (TIPM), utilizing ultrasound and serological markers. Data from patients at Mengchao Hepatobiliary Hospital and Fujian Provincial Cancer Hospital were analyzed, encompassing demographics, serological markers, and ultrasound findings, including tumor and peritumoral tissue stiffness changes pre- and post-treatment. The multivariate analysis revealed the neutrophil-to-lymphocyte ratio (NLR), ΔT (tumor stiffness change), tumor diameter, and albumin levels as independent predictors of therapy response. The TIPM model, integrating these factors, demonstrated superior predictive accuracy, validated by Receiver Operating Characteristic (ROC) curves, calibration curves, and decision curve analysis across both training and external validation cohorts. This predictive model stands to refine clinical decision-making, potentially improving treatment outcomes for advanced HCC patients by identifying those most likely to benefit from combined immunotherapy approaches.

Keywords Hepatocellular carcinoma, Advanced stage, Targeted therapy, Immunotherapy, Prediction model

Liver cancer remains a formidable challenge in oncology, with hepatocellular carcinoma (HCC) being the most common type[1,2]. Liver transplantation and tumor resection represent the cornerstone treatments for early-stage liver cancer, offering a potential cure for this debilitating disease[3]. Unfortunately, a significant proportion of patients are diagnosed at an advanced stage, where curative surgeries are no longer viable options[4]. For these patients, palliative treatments have been the primary recourse, providing limited hope for prolonged survival. In this context, combined targeted immunotherapy emerges as a groundbreaking therapeutic strategy, heralding a new era for the management of advanced liver cancer[5]. This innovative approach has shown promise in improving prognosis for patients with progressive liver cancer[6], albeit the overall benefit rate from such therapies remains modest. Identifying patients who are most likely to benefit from combined targeted and immunotherapy is, therefore, paramount, underscoring the need for precise predictive models.

Imaging modalities have played a pivotal role in diagnosing and managing liver cancer, with recent advancements significantly enhancing our ability to assess disease progression and response to treatment[7]. Other researchers have explored various imaging techniques, including MRI and CT scans, to predict the efficacy of cancer therapies[8,9]. These studies have laid the groundwork for integrating imaging biomarkers into therapeutic decision-making, although they often require expensive equipment and specialized expertise.

Ultrasonography, with its real-time imaging capabilities, repeatability, and lack of radiation exposure, has gained favor among clinicians, particularly with the recent development of an emerging technology: elastography. This technique is capable of reflecting the stiffness of tissues in the target area[10,11]. By dynamically measuring tissue stiffness, it can indicate the degree of response of the target area to treatment. Existing studies have confirmed that if TACE (Transarterial Chemoembolization) treatment is effective, tissue stiffness will decrease[12,13]. However, whether changes in tissue stiffness can predict the efficacy of targeted immunotherapy

[1]Department of Ultrasound, Mengchao Hepatobiliary Hospital of Fujian Medical University, Fuzhou 350025, P. R. China. [2]Department of PET, Mengchao Hepatobiliary Hospital of Fujian Medical University, Fuzhou 350025, P. R. China. [3]Department of Ultrasound, The First Affiliated Hospital, Fujian Medical University, Fuzhou 350001, P. R. China. [4]Department of Ultrasound, Binhai Campus of the First Affiliated Hospital, National Regional Medical Center, Fujian Medical University, Fuzhou 350001, P. R. China. ✉email: xjian_y@163.com

remains unexplored. Serological markers are easily obtained in clinical diagnosis and treatment, and research has shown that they hold significant importance in predicting the prognosis of targeted immunotherapy[14]. Nevertheless, the instability of serological markers has limited their widespread application. Therefore, it is uncertain whether combining ultrasonic indicators with serological markers can predict the effectiveness of targeted immunotherapy, and this paper seeks to verify this.

Results

Characteristics of all patients

This study included a total of 327 patients, with targeted immunotherapy being effective in 239 cases (73.1%) and noneffective in 88 cases (26.9%). Among these, the internal training cohort comprised 152 patients, the internal validation cohort 68 patients, and the external validation cohort 107 patients. No significant differences were observed across the various indicators in the three cohorts, indicating comparability (Table 1).

Characteristics in internal training cohort

In the internal training cohort, there were 110 cases of TIE and 42 cases of TIN. Differences were observed between the two groups in the following indicators: the proportion of NLR (neutrophil-to-lymphocyte ratio) < 3, the proportion of ΔT greater than 0, the proportion with satellite nodules, and levels of ALT (alanine aminotransferase), ALB (albumin), PLT (platelet count), GGT (gamma-glutamyl transferase), PT (prothrombin time), PTA (prothrombin activity), and tumor diameter. After excluding collinearity, indicators that showed differences in the univariate analysis were included in the subsequent multivariate analysis. The results indicated that NLR, ΔT, ALB, and Diameter are independent predictors of treatment outcome, as shown in Table 2. Additionally, we used a random forest model to rank the importance of each indicator, as illustrated in Fig. 1,2,3, demonstrating that the selected indicators are representative.

Model presentation

We constructed an ultrasound model using ΔT and Diameter, and a serological model using ALB and NLR. By integrating these four metrics, we created the Combined Model, known as the Target Immunotherapy Predict Model (TIPM). The Combined Model was visualized for presentation, as shown in Fig. 4.

ROC plotting

Subsequently, we plotted the ROC curves for the three models across various cohorts (internal training cohort, internal validation cohort, external validation cohort), as shown in Fig. 5, and calculated their AUCs. The AUCs of the models were then compared using the DeLong test. It was found that the Combined Model (TIPM) achieved the highest AUC across different cohorts with a significance level of $P < 0.05$. We utilized TIPM to calculate each patient's risk score, employing the Youden Index to find the optimal cutoff value. A threshold of 160 was used for categorization. Sensitivity, specificity, and other metrics were calculated across all cohorts, as indicated in Table 3.

Calibration plotting

We plotted the calibration curves for the three models across different cohorts, as illustrated in Fig. 6. The TIPM model was found to closely align with the true event curve (45° line) across all cohorts. The Hosmer and Lemeshow (H-L) P value and Brier score were calculated, with TIPM achieving the highest H-L P value and the lowest Brier score across different cohorts (as shown in Table 4). This indicates that TIPM has the highest calibration rate compared to the ultrasound and serological models.

Decision curve analysis plotting

The Decision Curve Analysis (DCA) for the three models were plotted across different cohorts, as shown in Fig. 7. TIPM was observed to be above the other models in different cohorts, indicating that using TIPM could provide greater net benefit for clinical decision-making.

Comparison of response evaluation systems

Among all patients, the overall response rates were 72.4%, 69.4%, and 71.2% according to mRECIST, RECIST 1.1, and iRECIST, respectively. The concordance between mRECIST and RECIST 1.1 was moderate ($\kappa = 0.68$), while the agreement between mRECIST and iRECIST was higher ($\kappa = 0.79$). These results suggest that mRECIST captured most, but not all, immune-related responses, and the addition of RECIST 1.1 and iRECIST increased the robustness and interpretability of treatment evaluation Fig. 8.

Association of TIPM score with clinical outcomes

The optimal cutoff value of the TIPM score was determined to be 160 based on the Youden index from receiver operating characteristic (ROC) analysis, which stratified patients into high- and low-risk groups. Kaplan–Meier analyses demonstrated that patients with high TIPM scores exhibited markedly poorer overall survival (OS) compared with those in the low-score group across all datasets. In the training cohort, the median OS was 142 days in the high-risk group versus 178 days in the low-risk group ($p < 0.0001$). In the internal validation cohort, median OS was 138 days versus 172 days ($p = 0.032$), and in the external validation cohort, 145 days versus 180 days ($p = 0.0019$)(Figure 8). These consistent findings indicate that a higher TIPM score is significantly associated with shorter survival duration and unfavorable clinical outcomes, confirming the model's robust predictive performance and reproducibility across independent cohorts.

	Total	Train	Test	External	*P*-value
Progression of disease					
TIE	239 (73.1%)	110 (72.4%)	53 (77.9%)	76 (71.0%)	0.59
TIN	88 (26.9%)	42 (27.6%)	15 (22.1%)	31 (29.0%)	
OS					
Live	239 (73.1%)	110 (72.4%)	53 (77.9%)	76 (71.0%)	0.59
Die	88 (26.9%)	42 (27.6%)	15 (22.1%)	31 (29.0%)	
NLR					
<=3	177 (54.1%)	84 (55.3%)	37 (54.4%)	56 (52.3%)	0.92
>3	150 (45.9%)	68 (44.7%)	31 (45.6%)	51 (47.7%)	
ΔT					
<0	145 (44.3%)	68 (44.7%)	26 (38.2%)	51 (47.7%)	0.48
>=0	182 (55.7%)	84 (55.3%)	42 (61.8%)	56 (52.3%)	
ΔP					
<0	263 (80.4%)	121 (79.6%)	56 (82.4%)	86 (80.4%)	0.92
>=0	64 (19.6%)	31 (20.4%)	12 (17.6%)	21 (19.6%)	
Statelite nodule					
Yes	301 (92.0%)	139 (91.4%)	63 (92.6%)	99 (92.5%)	0.96
No	26 (8.0%)	13 (8.6%)	5 (7.4%)	8 (7.5%)	
Sex					
Male	287 (87.8%)	133 (87.5%)	60 (88.2%)	94 (87.9%)	1
Female	40 (12.2%)	19 (12.5%)	8 (11.8%)	13 (12.1%)	
Echo of tumor					
Homogeneous	211 (64.5%)	92 (60.5%)	46 (67.6%)	73 (68.2%)	0.39
Heterogeneous	116 (35.5%)	60 (39.5%)	22 (32.4%)	34 (31.8%)	
Capsual of tumor					
Clear	40 (12.2%)	21 (13.8%)	5 (7.4%)	14 (13.1%)	0.4
Obscure	287 (87.8%)	131 (86.2%)	63 (92.6%)	93 (86.9%)	
Collateral circulation					
No	244 (74.6%)	110 (72.4%)	57 (83.8%)	77 (72.0%)	0.14
Yes	83 (25.4%)	42 (27.6%)	11 (16.2%)	30 (28.0%)	
AFP					
<200	120 (36.7%)	58 (38.2%)	26 (38.2%)	36 (33.6%)	0.74
>200	207 (63.3%)	94 (61.8%)	42 (61.8%)	71 (66.4%)	
Macrovascular invansion					
No	121 (37.0%)	61 (40.1%)	25 (36.8%)	35 (32.7%)	0.47
Yes	206 (63.0%)	91 (59.9%)	43 (63.2%)	72 (67.3%)	
Viral hepatitis					
Non-HBV	37 (11.3%)	19 (12.5%)	3 (4.4%)	15 (14.0%)	0.1
HBV	290 (88.7%)	133 (87.5%)	65 (95.6%)	92 (86.0%)	
Age(years)	51.2 ± 9.5	50.7 ± 9.2	53.6 ± 10.4	50.5 ± 9.3	0.076
ALT(U/L)	108.6 ± 371.4	138.1 ± 535.2	78.1 ± 92.2	86.1 ± 92.0	0.41
AST(U/L)	80.1 ± 63.4	82.3 ± 63.6	74.2 ± 62.8	80.8 ± 64.0	0.68
PLT(/L)	238.0 ± 68.9	241.3 ± 72.0	220.1 ± 59.1	244.6 ± 68.8	0.051
ALB(g/L)	39.8 ± 14.3	38.9 ± 5.4	43.4 ± 29.4	38.9 ± 5.3	0.073
GGT(u/L)	335.0 ± 398.9	358.6 ± 432.9	288.4 ± 280.1	331.2 ± 413.0	0.48
TBIL(umol/L)	35.0 ± 51.1	36.4 ± 53.9	30.3 ± 44.1	36.1 ± 51.5	0.69
ALP(mmol/L)	305.4 ± 271.7	306.4 ± 244.4	273.8 ± 261.7	324.2 ± 312.6	0.49
PT(s)	12.2 ± 0.9	12.1 ± 0.9	12.2 ± 0.8	12.2 ± 0.9	0.62

Continued

	Total	Train	Test	External	*P*-value
PTA(%)	110.9 ± 22.1	111.7 ± 23.3	107.6 ± 17.2	112.0 ± 22.9	0.38
INR	1.0 ± 0.3	1.0 ± 0.3	1.0 ± 0.2	1.1 ± 0.4	0.088
BMI	22.8 ± 2.8	23.0 ± 2.8	22.3 ± 2.8	23.0 ± 2.9	0.27
Diameter(cm)	8.4 ± 1.5	8.4 ± 1.5	8.5 ± 1.4	8.2 ± 1.5	0.53
Ostime(days)	132.3 ± 56.0	129.3 ± 58.7	133.7 ± 52.4	135.8 ± 54.4	0.63

Table 1. Basic characteristics in all patients. TIE: target and immunotherapy effective; TIN: target and immunotherapy noneffective; ΔT: The difference in stiffness of the tumor six weeks after treatment minus the stiffness before treatment.ΔP: The difference in stiffness of the surrounding tissue six weeks after treatment minus the stiffness before treatment.

Subgroup analysis according to viral etiology

To investigate whether the predictive efficacy of the TIPM model differed according to viral etiology, patients were stratified into HBV ($n = 290$, 88.7%) and non-HBV ($n = 37$, 11.3%) subgroups. Across both subgroups, patients with higher TIPM scores demonstrated significantly shorter overall survival (OS) compared with those in the low-TIPM group.In the HBV-related HCC subgroup, the median OS was 118 days in the high-TIPM group versus 160 days in the low-TIPM group (log-rank $p = 0.018$; HR = 2.21, 95% CI 1.15–4.27). In the non-HBV HCC subgroup, a similar pattern was observed, with a median OS of 125 days in the high-TIPM group versus 171 days in the low-TIPM group (log-rank $p = 0.042$; HR = 2.47, 95% CI 1.03–5.93).No significant interaction was detected between viral status and TIPM score (p for interaction = 0.56), indicating that the prognostic value of the TIPM model was consistent regardless of HBV infection. These findings confirm that the model preserves predictive robustness across different etiological backgrounds within a 185-day observation period.

Discussion

Our study's retrospective analysis provides critical insights into the predictive markers for the efficacy of targeted combined immunotherapy in advanced HCC patients. We identified four independent risk factors: NLR, tumor diameter, ΔT, and album levels, then we construct a predict model TIPM, which show good predicted performance. Our study may have important implications for personalized treatment.

The Neutrophil-to-Lymphocyte Ratio (NLR) has emerged as a significant biomarker for evaluating the efficacy of immunotherapies in cancer treatment. Elevated NLR values are indicative of a systemic inflammatory response, which has been consistently associated with adverse effects on the tumor microenvironment and a diminished response to immune checkpoint inhibitors (ICIs) across various cancer types. Studies have demonstrated that patients with higher NLR values exhibit significantly poorer overall survival, progression-free survival, and lower rates of response and clinical benefit from ICIs, underscoring the crucial role of systemic inflammation in the modulation of tumor immunotherapy outcomes[15]. This correlation between NLR and treatment efficacy is further substantiated by the observation of heterogeneity in response across different studies, which underscores the importance of adjusting for prognostic factors and suggests a complex interaction between systemic inflammatory markers and cancer prognosis[16].The predictive value of NLR, alongside other biomarkers such as Tumor Mutational Burden (TMB), offers a nuanced approach to patient stratification and treatment planning, advocating for the integration of systemic inflammation assessment in the decision-making process to optimize immunotherapy strategies[15] .

The size of a tumor, as measured by Its diameter, Is a critical factor In evaluating the biological aggressiveness of cancer and has significant implications for predicting the efficacy of treatment. Larger tumors often indicate a worse prognosis due to their potential for advanced disease progression and reduced responsiveness to therapeutic interventions. This correlation highlights the importance of tumor diameter as a key predictive measure of treatment efficacy, underscoring its role in guiding clinical decisions regarding cancer management. Advancements in imaging technologies, such as magnetic resonance imaging (MRI), have significantly improved the accuracy of tumor size evaluation, making it possible to assess treatment response with greater precision. MRI, in particular, offers detailed insights into tumor morphology, hemodynamics, and metabolism, allowing for early and comprehensive evaluation of the response to neoadjuvant chemotherapy (NAC). Studies have confirmed that changes in tumor volume and diameter, as observed through MRI, are among the most accurate indicators of pathological response following treatment. This is especially true for breast cancer NAC, where reducing tumor volume has been identified as the most reliable indicator of pathological response, followed closely by changes in tumor diameter[17].

Furthermore, the association between baseline tumor size and outcomes in cancer treatment has been substantiated by various studies. For instance, baseline tumor size has been identified as an independent prognostic factor for overall survival in patients with melanoma treated with pembrolizumab, emphasizing its predictive value beyond traditional staging criteria[18] . Similar findings have been observed in non-small cell lung cancer (NSCLC), where baseline tumor size was found to be a predictive and prognostic factor for patients treated with immune checkpoint inhibitors, suggesting that tumor size may significantly influence the effectiveness of immuno-oncological treatments[18].These insights into the role of tumor diameter in predicting treatment efficacy underscore the necessity of incorporating tumor size evaluations into treatment planning and prognosis assessment. As such, tumor diameter serves not only as a marker of cancer's biological behavior but also as a crucial component of personalized treatment strategies aimed at optimizing therapeutic outcomes.

	Total	TIE	TIN	*P*-value	β	OR	95%CI		*P*-value
							Lower	Upper	
NLR					2.146	2.616	0.665	3.941	0.009
<=3	84 (55.3%)	71 (64.5%)	13 (31.0%)	< 0.001					
>3	68 (44.7%)	39 (35.5%)	29 (69.0%)						
ΔT					-3.845	-4.311	-5.881	-2.301	< 0.001
<0	68 (44.7%)	33 (30.0%)	35 (83.3%)	< 0.001					
>=0	84 (55.3%)	77 (70.0%)	7 (16.7%)						
ΔP									
<0	121 (79.6%)	85 (77.3%)	36 (85.7%)	0.37					
>=0	31 (20.4%)	25 (22.7%)	6 (14.3%)						
Statelite nodule					1.386	1.231	-0.751	3.712	0.218
Yes	139 (91.4%)	106 (96.4%)	33 (78.6%)	0.001					
No	13 (8.6%)	4 (3.6%)	9 (21.4%)						
Sex									
Male	133 (87.5%)	95 (86.4%)	38 (90.5%)	0.59					
Female	19 (12.5%)	15 (13.6%)	4 (9.5%)						
Echo of tumor									
Homogeneous	92 (60.5%)	67 (60.9%)	25 (59.5%)	1					
Heterogeneous	60 (39.5%)	43 (39.1%)	17 (40.5%)						
Capsual of tumor									
Clear	21 (13.8%)	12 (10.9%)	9 (21.4%)	0.12					
Obscure	131 (86.2%)	98 (89.1%)	33 (78.6%)						
Collateral circulation									
No	110 (72.4%)	82 (74.5%)	28 (66.7%)	0.42					
Yes	42 (27.6%)	28 (25.5%)	14 (33.3%)						
AFP									
<200	58 (38.2%)	45 (40.9%)	13 (31.0%)	0.35					
>200	94 (61.8%)	65 (59.1%)	29 (69.0%)						
Macrovascular invansion									
No	61 (40.1%)	46 (41.8%)	15 (35.7%)	0.58					
Yes	91 (59.9%)	64 (58.2%)	27 (64.3%)						
Viral hepatitis									
Non-HBV	19 (12.5%)	12 (10.9%)	7 (16.7%)	0.41					
HBV	133 (87.5%)	98 (89.1%)	35 (83.3%)						
Age(years)	50.7 ± 9.2	50.5 ± 9.7	51.2 ± 7.9	0.81					
ALT(U/L)	138.1 ± 535.2	160.9 ± 624.8	78.6 ± 110.6	0.036	-0.001	-0.43	-0.008	0.001	0.667
AST(U/L)	82.3 ± 63.6	80.4 ± 62.0	87.1 ± 68.2	0.32					
PLT(/L)	241.3 ± 72.0	256.9 ± 62.1	200.4 ± 80.6	< 0.001	-0.003	-0.554	-0.016	0.008	0.58
ALB(g/L)	38.9 ± 5.4	40.0 ± 5.5	36.1 ± 3.8	< 0.001	-0.246	-3.011	-0.421	-0.097	0.003
GGT(u/L)	358.6 ± 432.9	407.7 ± 489.6	230.2 ± 172.2	0.019	-0.001	-1.405	-0.004	0	0.16
TBIL(umol/L)	36.4 ± 53.9	32.9 ± 54.7	45.6 ± 51.1	0.23					
ALP(mmol/L)	306.4 ± 244.4	306.1 ± 256.4	307.3 ± 212.8	0.64					
PT(s)	12.1 ± 0.9	12.0 ± 0.9	12.5 ± 1.0	0.014	0.553	1.615	-0.13	1.237	0.106
PTA(%)	111.7 ± 23.3	115.1 ± 23.9	102.7 ± 19.5	0.004					
INR	1.0 ± 0.3	1.0 ± 0.1	1.1 ± 0.5	0.033					
BMI	23.0 ± 2.8	23.0 ± 2.7	22.8 ± 2.9	0.63					
Diameter(cm)	8.4 ± 1.5	8.0 ± 1.3	9.6 ± 1.5	< 0.001	0.674	2.094	0.084	1.36	0.036

Table 2. Univariate and multivariate analysis in training cohort. TIE: target and immunotherapy effective; TIN: target and immunotherapy noneffective; ΔT: The difference in stiffness of the tumor six weeks after treatment minus the stiffness before treatment.ΔP: The difference in stiffness of the surrounding tissue six weeks after treatment minus the stiffness before treatment.

Incorporating the changes in tumor tissue stiffness (ΔT) as an indicator of treatment effectiveness, recent advances in imaging technologies such as Contrast-Enhanced Ultrasound (CEUS) and Ultrasound Elastography have provided valuable insights into assessing the response of tumors to neoadjuvant chemotherapy (NAC). Ultrasound elastography, which measures changes in tissue stiffness, has emerged as a significant method for

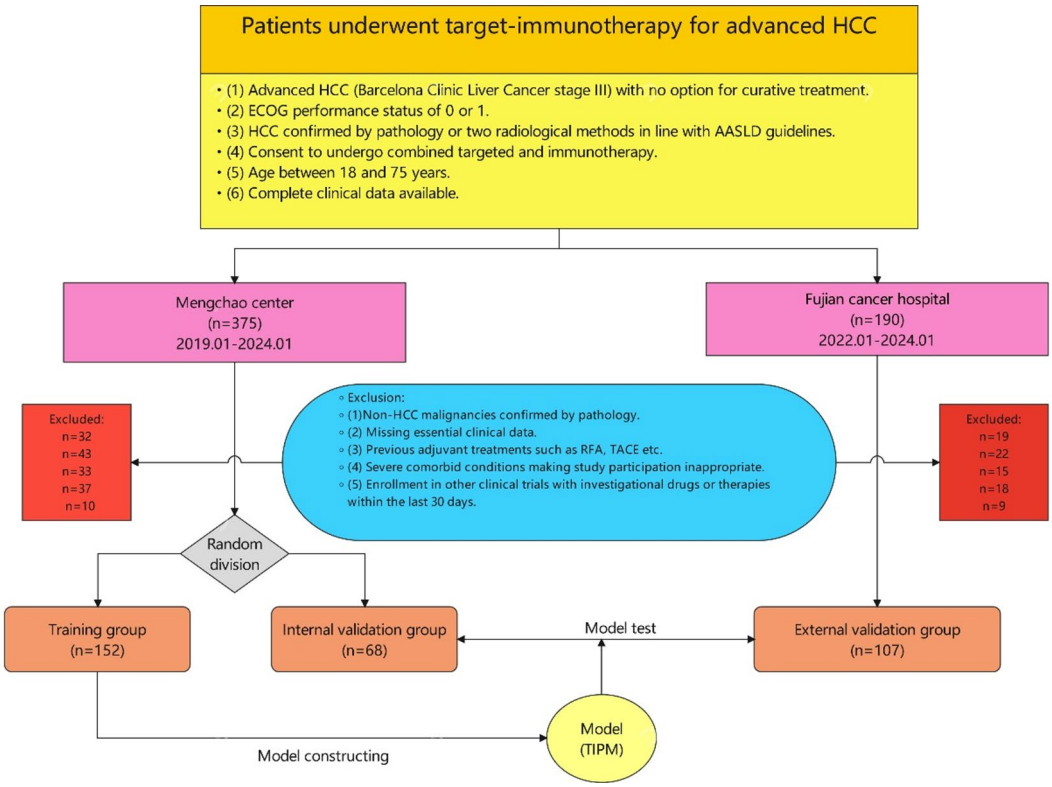

Fig. 1. Case inclusion flowchart.

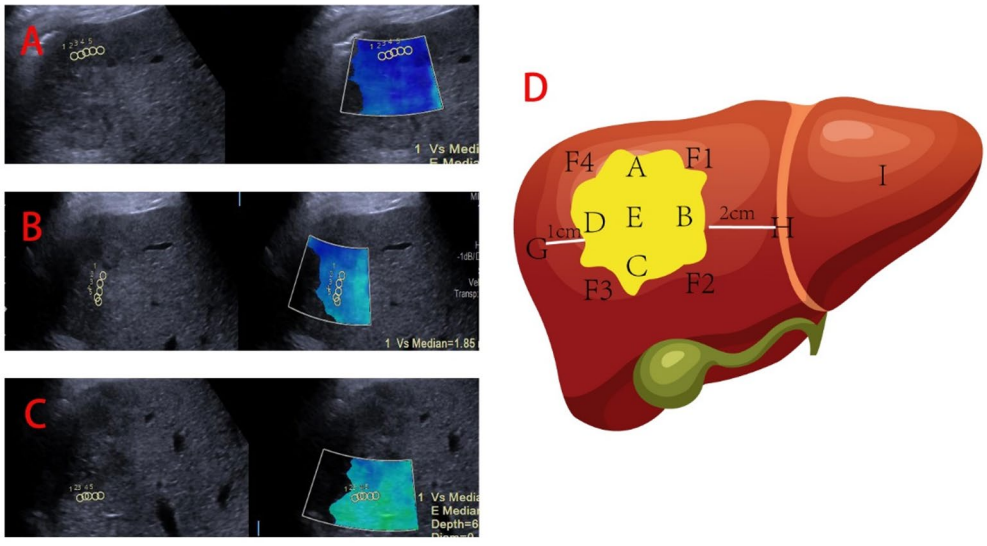

Fig. 2. Diagrams illustrating tumor stiffness measurements (**A**) demonstrates measuring the stiffness in front of the tumor, (**B**) shows measuring the stiffness on the left side of the tumor, (**C**) indicates measuring the stiffness at the bottom of the tumor, and (**D**) depicts the positions for measuring tumor stiffness, including the anterior, posterior, left, right, and middle (ABCDE) of the tumor parenchyma, the stiffness of the liver tissue in the four quadrants adjacent to the tumor parenchyma (F1, F2, F3, F4), the tissue stiffness one centimeter from the tumor edge (**G**), two centimeters from the tumor edge (**H**), and the stiffness of normal liver tissue (**I**).

evaluating NAC efficacy. This technique, through both strain elastography (SE) and shear wave elastography (SWE), offers qualitative and quantitative analyses of tissue softness and stiffness. Studies have shown that SE can predict NAC response with high sensitivity and specificity after just two treatment cycles. Moreover, SWE has been found to significantly associate the relative change of tumor stiffness after two NAC cycles with the

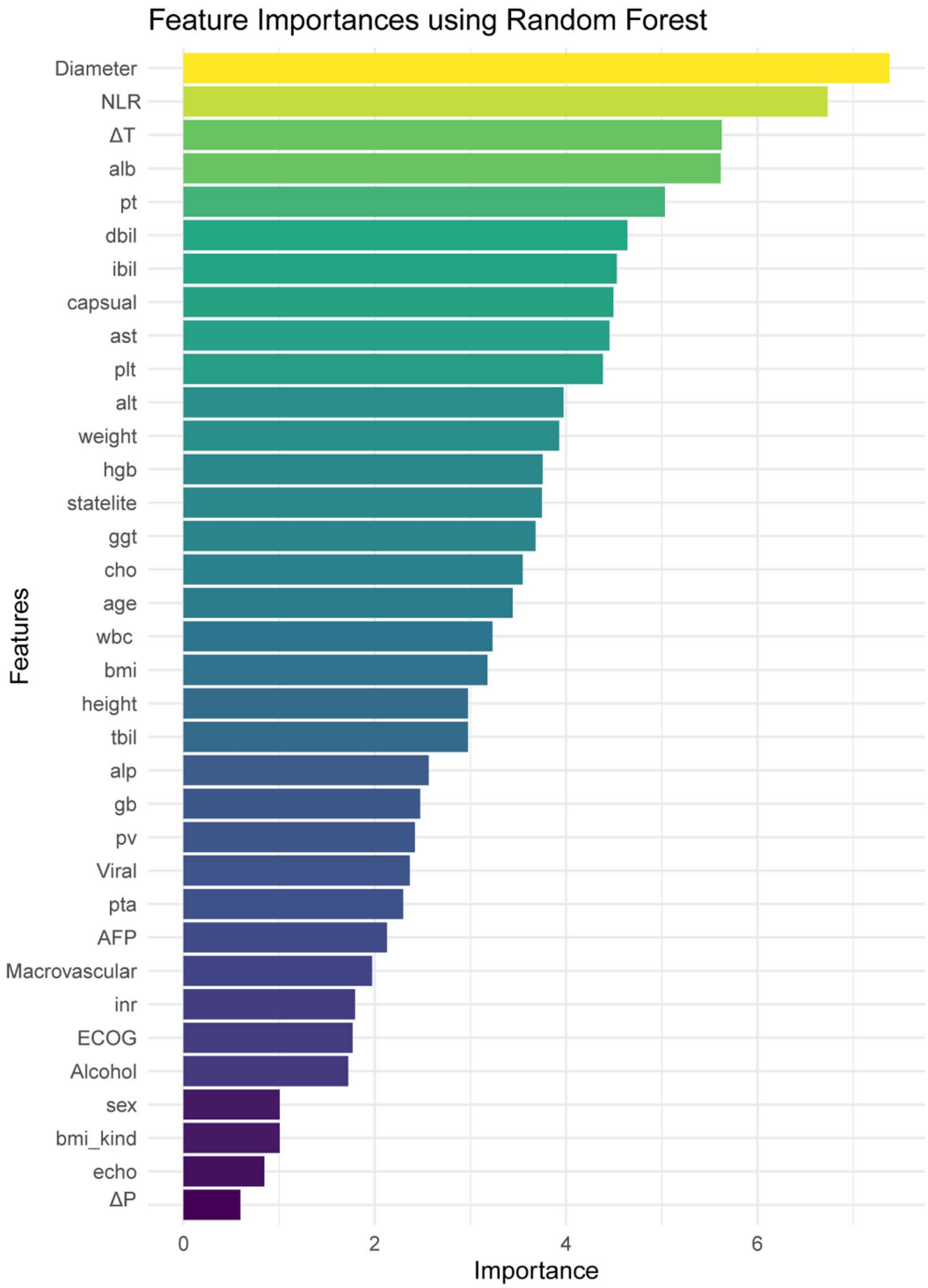

Fig. 3. Importance ranking chart for included features: Displays Diameter, NLR, and T ALB as having the highest importance.

pathological response of postoperative specimens, providing a new predictive parameter for judging the efficacy of NAC for breast cancer[19]. In HCC, stiffness reduction ($\Delta T > 0$) may reflect immune infiltration, fibrosis modulation, or tumor necrosis induced by immunotherapy, as supported by multi-omics studies linking matrix stiffness to immune response[20]. The effectiveness of these imaging techniques in evaluating changes in tumor tissue stiffness underscores the complexity of tumor response to treatments. By offering insights Into the physical properties of tumors, such as elasticity and stiffness, these methods contribute significantly to our understanding of how tumors respond to therapies. They also highlight the potential for integrating imaging findings with

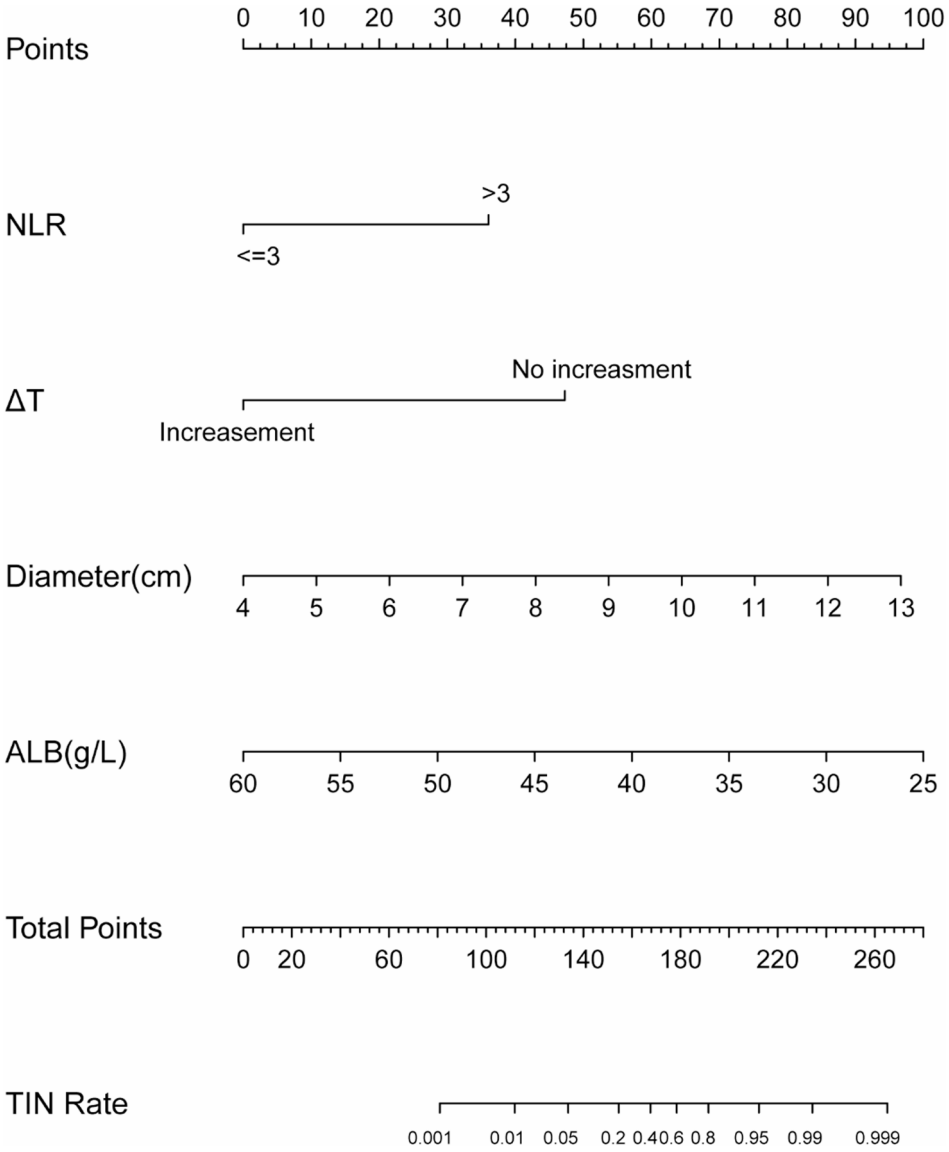

Fig. 4. Nomogram: Presents the modeling cohort for the Target Immunotherapy Predict Model (TIPM).

clinical and biological indicators to enhance the precision of treatment effectiveness evaluations[21]. Future studies with paired biopsies are warranted to correlate ΔT with histopathological changes.

Lower albumin levels have been extensively studied and found to reflect poor overall patient health status, impacting outcomes from targeted immunotherapies across various cancer types. Serum albumin serves not only as a marker for general health but also has a prognostic and predictive value in patients undergoing immune checkpoint blockade (ICB) therapy. Studies have shown that high serum albumin levels are associated with better overall survival (OS) and progression-free survival (PFS) in patients treated with ICB across multiple cancer types, including melanoma and non-small cell lung cancer (NSCLC)[22]. Moreover, albumin levels have been linked to the body's inflammatory status and nutritional health, which are crucial in the context of cancer treatment. Specifically, higher albumin levels indicate a lower systemic inflammatory state and better nutritional status, which are conducive to a more favorable response to immunotherapy[22,23]. The dose-dependent relationship observed between serum albumin levels and clinical responses to ICB therapy further underscores the importance of maintaining optimal albumin levels for enhancing treatment outcomes[23]. In the realm of metastatic NSCLC, hypoalbuminemia has been identified as a biomarker indicative of resistance to first-line treatments, further emphasizing the role of albumin in predicting treatment outcomes[24]. The significant association between pretreatment albumin levels and OS, demonstrated through Kaplan-Meier survival analyses and Cox's proportional-hazards models, indicates that serum albumin could serve as a critical factor in stratifying patients for ICB therapy[24]. Furthermore, the clinical significance of the serological biomarkers identified in this study aligns with the international consensus on immunotherapy biomarkers. According to the 2025 Society for Immunotherapy of Cancer (SITC) consensus statement on essential biomarkers for immunotherapy clinical protocols, peripheral blood–based indicators such as the neutrophil-to-lymphocyte ratio (NLR), albumin, and

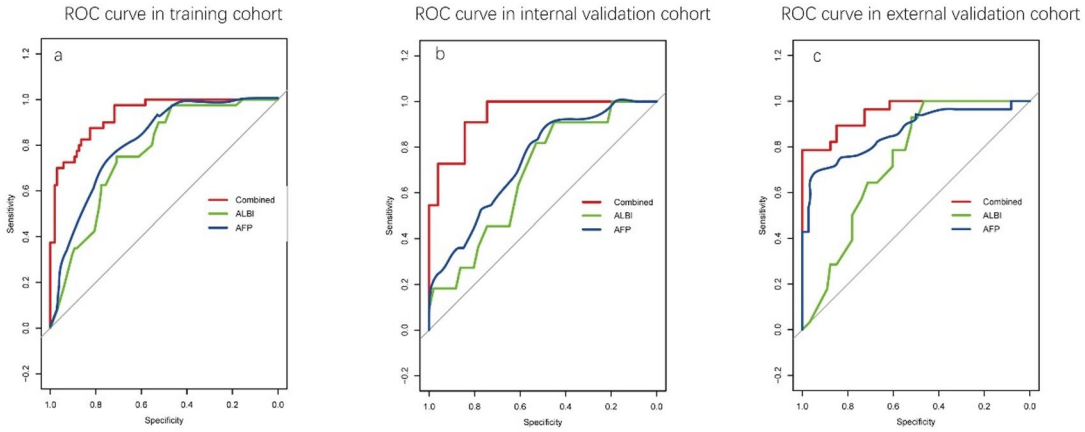

Fig. 5. ROC curves: (**A**) showing the ROC curves for various models in the internal training cohort. (**B**) showing the ROC curves for various models in the internal validation cohort. (**C**) showing the ROC curves for various models in the external validation cohort. In all cohorts, the TIPM model exhibits the largest area under the curve.

	Training cohort	Internal cohort	External cohort
Sensitivity(%)	82.5	81.82	82.14
Specificity(%)	85.44	84.31	87.67
Accuracy(%)	84.62	83.87	86.14
Precision(%)	68.75	52.94	71.88
F1 score(%)	75	64.29	76.67

Table 3. Assessment measures for all cohorts.

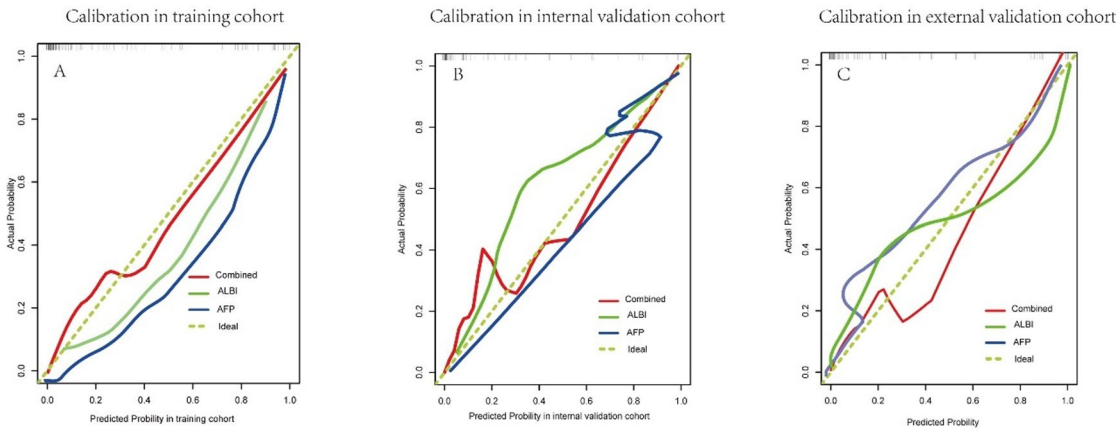

Fig. 6. Calibration curves: (**A**) showing the Calibration curves for various models in internal training cohort. (**B**) showing the Calibration curves for various models in internal validation cohort. (**C**) showing the Calibration curves for various models in external validation cohort.In all these cohorts, the TIPM model is shown to be distributed around the 45° line, indicating high accuracy of the TIPM.

lactate dehydrogenase (LDH) are recognized as essential biomarkers reflecting systemic immune–inflammatory and nutritional status. These biomarkers are recommended for inclusion in all immunotherapy-related clinical trials due to their strong biological relevance, feasibility, and prognostic value across tumor types. The incorporation of NLR and ALB into our TIPM model therefore conforms to this international framework, highlighting the translational potential of these easily accessible biomarkers for predicting immunotherapy efficacy in advanced HCC[25].

Our study expands upon previous research by further validating the importance of serological and ultrasonography indicators in predicting responses to targeted combined immunotherapy in patients with

		AUC	95%CI		Hosmer and Lemeshow P value	Brier score
			Lower	Upper		
Training cohort	Combined	0.933	0.893	0.973	0.8398	0.00907
	ALBI	0.755	0.671	0.835	0.155	0.185
	AFP	0.642	0.551	0.764	0.105	0.128
Internal validation	Combined	0.941	0.879	0.963	0.9921	0.0695
	ALBI	0.712	0.626	0.821	0.3598	0.1574
	AFP	0.602	0.514	0.762	0.4856	0.099
External validation	Combined	0.937	0.864	0.972	0.5663	0.0714
	ALBI	0.852	0.648	0.911	0.0356	0.2057
	AFP	0.824	0.628	0.902	0.0457	0.0682

Table 4. AUC/Hosmer and lemeshow/Brier score in all cohorts.

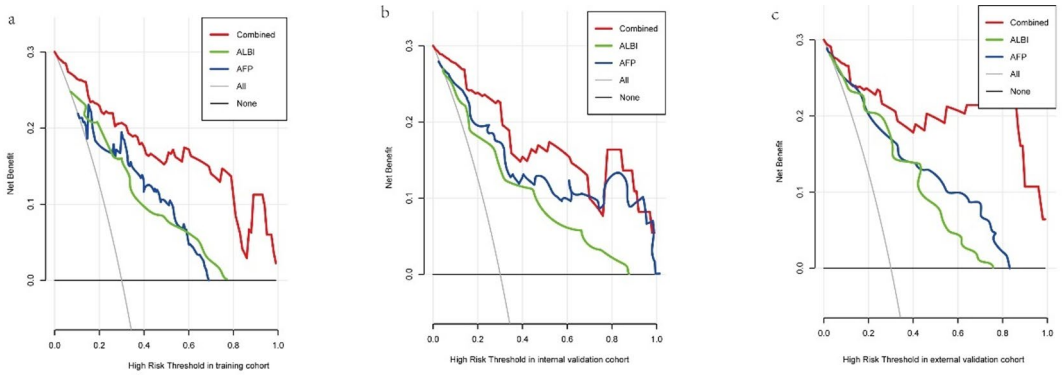

Fig. 7. DCA curves: (**A**) showing the DCA curves for various models in internal training cohort. (**B**) showing the DCA curves for various models in internal validation cohort. (**C**) showing the DCA curves for various models in external validation cohort. In all cohorts, the TIPM model is positioned above other models (ultrasound model, serological r model) towards the upper right of the graph, meaning the TIPM can provide the maximum clinical net benefit to patients.

advanced hepatocellular carcinoma (HCC). Previous studies laid the groundwork by focusing primarily on single predictive factors or analyzing smaller patient cohorts. In contrast, our research takes a more comprehensive approach, incorporating multiple predictive factors and applying these models to a larger cohort of patients. This broader perspective allows for a more nuanced understanding of the complex interplay between various biomarkers and their predictive value in the context of HCC immunotherapy[26,27].

Additionally, the revolutionizing role of contrast-enhanced ultrasound (CEUS) and serological indicators in early recurrence prediction postoperatively for HCC patients further exemplifies the advancements in surveillance methodologies. These techniques enhance our ability to monitor and predict treatment outcomes, providing valuable insights into the effectiveness of therapeutic interventions[28].Our study not only corroborates the utility of serological and ultrasonography indicators in forecasting immunotherapy responses in advanced HCC but also highlights the evolving landscape of HCC treatment strategies. By integrating these predictive models with current knowledge on the immune microenvironment and the latest advances in immunotherapy, we can better tailor treatments to individual patients, ultimately improving clinical outcomes.

The clinical application potential"of p̈edictive models for HCC is underscored by research indicating their utility in guiding clinical decisions, tailoring personalized treatment plans, and optimizing cancer treatments based on comprehensive risk and prognosis assessments. Nomograms, derived from large-scale databases like SEER, have demonstrated strong predictive abilities for all-cause and cancer-specific early death, offering a promising tool for clinicians to enhance survival outcomes for HCC patients. However, limitations such as retrospective study design and the specificity of data sources like the SEER database to the US population suggest the need for further validation and global research to refine these models[29]. Therefore, we developed TIPM, a predictive model suitable for Chinese population characteristics.

Limitations

This study has several limitations. First, its retrospective nature inevitably introduces potential selection bias and unmeasured confounding factors, such as variations in prior systemic therapies, comorbidities, and exclusion of patients with incomplete records. These issues may affect the observed associations between biomarkers and treatment outcomes.Second, because the cohort primarily included patients with advanced-stage, unresectable HCC, histological subtyping and detailed baseline liver conditions (e.g., cirrhosis, NAFLD) could not be

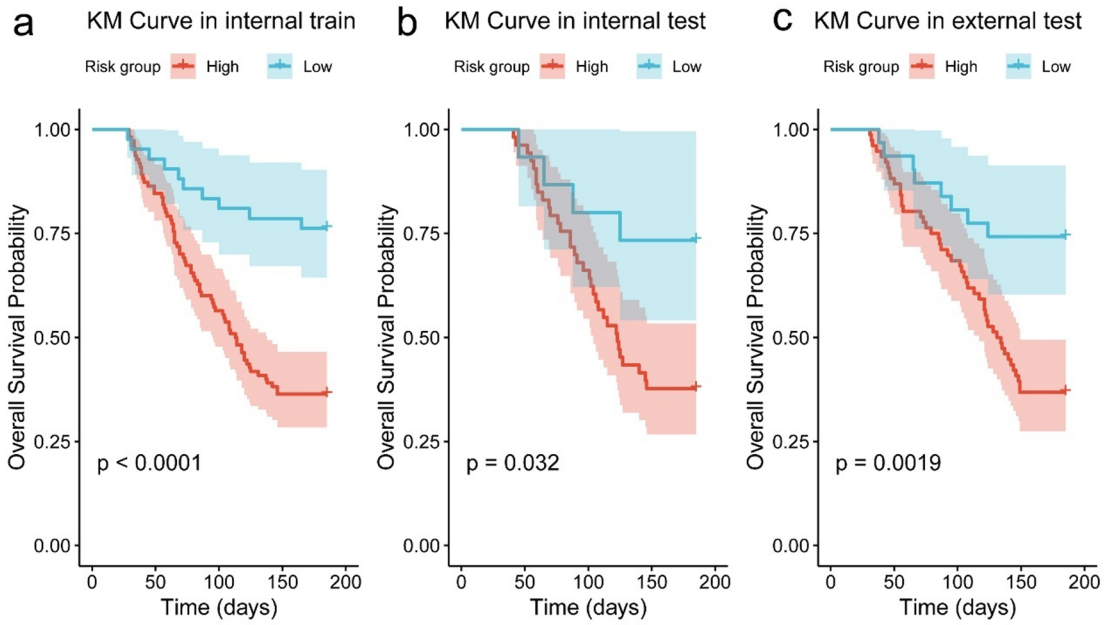

Fig. 8. Kaplan–Meier survival curves for overall survival (OS) in the training, internal validation, and external validation cohorts. (**A**) In the training cohort, patients in the high-risk group exhibited significantly poorer OS compared with those in the low-risk group ($p < 0.0001$). (**B**) A similar trend was observed in the internal validation cohort ($p = 0.032$).C Consistent results were also found in the external validation cohort ($p = 0.0019$).

comprehensively collected, which may limit data completeness.Third, the ΔT parameter, representing dynamic stiffness alterations, was defined as a categorical integration of multi-point stiffness changes (≥ 5 of 9 intra- and peri-tumoral sites showing increased stiffness) rather than a single continuous value. This design aimed to capture the regional heterogeneity of tumor–peritumor stiffness distribution. However, such a definition precludes direct continuous correlation analysis with therapeutic response. Future work will refine quantitative stiffness mapping to enable continuous-variable evaluation and facilitate cross-center comparability.Moreover, the ΔT threshold (ΔT > 0 in ≥ 5/9 intra- and peri-tumoral sites) was empirically determined based on pilot observations rather than standardized criteria, and although identical Siemens Sequoia systems and unified operator training were used across centers, minor variations in probe handling or patient cooperation could not be entirely excluded. Future prospective studies should therefore aim to further standardize and externally validate elastography protocols to enhance reproducibility. Additionally, although the sample size was moderate, it may still limit statistical power and generalizability. The absence of a prospective validation cohort also restricts the real-world extrapolation of the proposed TIPM model. Future studies should therefore include multicenter, prospective validation to confirm its predictive robustness and clinical utility, following the approach highlighted by Piao et al. [30], who demonstrated that prospective design can effectively minimize confounding and strengthen causal inference.

Moreover, the biological mechanisms underlying the prognostic value of NLR and ΔT require further mechanistic exploration to refine predictive accuracy. Finally, detailed subgroup analyses stratified by etiology, liver function, and treatment regimen are warranted to facilitate more personalized and clinically applicable therapeutic strategies. Addressing these aspects will enhance the robustness, reproducibility, and translational potential of future research on hepatocellular carcinoma management.

This study has several limitations. First, its retrospective nature inevitably introduces potential selection bias and unmeasured confounding factors, such as variations in prior systemic therapies, comorbidities, and exclusion of patients with incomplete records. These issues may affect the observed associations between biomarkers and treatment outcomes. Second, because the cohort primarily included patients with advanced-stage, unresectable HCC, histological subtyping and detailed baseline liver conditions (e.g., cirrhosis, NAFLD) could not be comprehensively collected, which may limit data completeness. Third, the ΔT threshold (ΔT > 0 in ≥ 5/9 intra- and peri-tumoral sites) was empirically determined based on pilot observations rather than standardized criteria, and although identical Siemens Sequoia systems and unified operator training were used across centers, minor variations in probe handling or patient cooperation could not be entirely excluded. Future prospective studies should therefore aim to further standardize and externally validate elastography protocols to enhance reproducibility.

Additionally, although the sample size was moderate, it may still limit statistical power and generalizability. The absence of a prospective validation cohort also restricts the real-world extrapolation of the proposed TIPM model. Future studies should therefore include multicenter, prospective validation to confirm its predictive robustness and clinical utility, following the approach highlighted by Piao et al. [30], who demonstrated that prospective design can effectively minimize confounding and strengthen causal inference. Moreover, the

biological mechanisms underlying the prognostic value of NLR and ΔT require further mechanistic exploration to refine predictive accuracy. Finally, detailed subgroup analyses stratified by etiology, liver function, and treatment regimen are warranted to facilitate more personalized and clinically applicable therapeutic strategies. Addressing these aspects will enhance the robustness, reproducibility, and translational potential of future research on hepatocellular carcinoma management.

Conclusion

In conclusion, our study presents a robust framework for predicting the efficacy of targeted combined immunotherapy in advanced HCC patients, leveraging both serological and ultrasonography indicators. The independent risk factors identified offer a valuable guide for clinicians in selecting appropriate patients for treatment, potentially leading to improved patient outcomes and optimized treatment strategies.

Methods

Patients

This article presents a retrospective study conducted on patients suffering from advanced hepatocellular carcinoma (HCC), who were treated with a combination of targeted therapy and immunotherapy at Mengchao Hepatobiliary Hospital from January 1, 2019, to January 1, 2024, and at Fujian Provincial Cancer Hospital from January 1, 2022, to January 1, 2024. The study received ethical approval from the Mengchao Hepatobiliary Hospital Ethics Committee (Approval No. 2021_084_01). Informed consent was obtained from all subjects. Furthermore, all procedures performed in this study adhered strictly to the relevant guidelines and regulations, in alignment with the principles of the Declaration of Helsinki. The procedural flowchart of the study is illustrated in Fig. 1.

Inclusion criteria:

(1) Advanced HCC (Barcelona Clinic Liver Cancer stage III) with no option for curative treatment.
(2) ECOG performance status of 0 or 1.
(3) HCC confirmed by pathology or two radiological methods in line with AASLD guidelines.
(4) Consent to undergo combined targeted and immunotherapy.
(5) Complete clinical data available.

Exclusion criteria:

(1) Non-HCC malignancies confirmed by pathology.
(2) Missing essential clinical data.
(3) Prior systemic therapy for HCC (TACE, RFA and so on).
(4) Severe comorbid conditions making study participation inappropriate.
(5) Enrollment in other clinical trials with investigational drugs or therapies within the last 30 days.

Response evaluation (mRECIST, RECIST 1.1, and iRECIST)

Magnetic resonance imaging (MRI, 3.0 T; Siemens, Germany) was performed to evaluate treatment response. Arterial, portal venous, and delayed phase images were obtained at baseline and then monthly until week 26 or until patient death. Two experienced radiologists independently reviewed all imaging data, and any disagreement was resolved through consensus with a senior chief radiologist.

The primary assessment of tumor re”pons' was based on mRECIST criteria, which evaluate changes in viable (enhancing) tumor components. Patients were classified into the target and immunotherapy effective (TIE) group—including complete response (CR), partial response (PR), and stable disease (SD)—or the target and immunotherapy noneffective (TIN) group—defined as progressive disease (PD). According to mRECIST:

6 CR: Disappearance of all intratumoral arterial enhancement in all target lesions.
7 PR: At least a 30% decrease in the sum of diameters of viable (enhancing) target lesions compared with baseline.
8 SD: Neither sufficient shrinkage to qualify for PR nor sufficient increase to qualify for PD.
9 PD: At least a 20% increase in the sum of diameters of viable (enhancing) target lesions, taking as reference the smallest sum recorded since treatment initiation.

To enhance the robustness and comparability of response evaluation, all patients were further assessed using RECIST 1.1 and, where serial follow-up scans were available, iRECIST criteria.

Under RECIST 1.1, the sum of the longest diameters of up to five target lesions (maximum of two per organ) was measured. Treatment responses were categorized as:

- CR: Disappearance of all target lesions;
- PR: At least a 30% decrease in the sum of the longest diameters;
- SD: Neither PR nor PD criteria met;
- PD: At least a 20% increase in the sum of diameters, taking as reference the smallest sum on study.

Under iRECIST, patients who exhibited initial progression on imaging were categorized as immune unconfirmed progressive disease (iUPD) and were re-evaluated after ≥4 weeks. If further enlargement or new lesions were observed, the status was confirmed as immune confirmed progressive disease (iCPD); otherwise, the response was reclassified as iSD or iPR.

The final tumor response for each patient was determined by consensus and recorded under all three evaluation systems. These parallel criteria were applied to assess the consistency and robustness of response classification across different imaging frameworks.

Serology indexes

Fasting serology indices were meticulously collected during the morning hours to ensure the reliability of the data. The recorded parameters included a comprehensive spectrum of biochemical and hematological markers: Alanine Aminotransferase (ALT), Aspartate Aminotransferase (AST), Platelet Count (PLT), Absolute Neutrophil Count (ANC), Absolute Lymphocyte Count (ALC), Lactate Dehydrogenase (LDH), Albumin (ALB), Glutathione S-Transferase (GST), Total Bilirubin (TBIL), Creatinine (Cr), Alkaline Phosphatase (ALP), Prothrombin Time (PT), Prothrombin Time Activity (PTA), International Normalized Ratio (INR), along with serological markers for Hepatitis B Virus (HBV) and Hepatitis C Virus (HCV), including both antigens and antibodies. Additionally, Alpha Fetoprotein (AFP) levels were quantified. To further elucidate the inflammatory and immunological status of the subjects, the Neutrophil to Lymphocyte Ratio (NLR) was calculated. These indices provide a holistic view of the patients' biochemical and hematological health status, contributing significantly to our understanding of the underlying pathophysiological mechanisms.

Demographic information

Patients height, weight, gender, age were recorded pretreatment, calculate body mass index (BMI).

Therapeutic schedule

Immunotherapy use camrelizumab (airuika, Shengdiya): 3 mg/kg, intravenous injection once every 3 weeks until disease progression or intolerable toxicity.

Target therapy use lenvatinib Mesilate Capsules (leweima, weicai): Patients with weight < 60 kg, 8 mg, once a day; patients with weight ≥ 60 kg, 12 mg, once a day. Treatment should continue until the disease progresses or intolerable toxicity.

Ultrasound examination

Ultrasound examinations were performed using identical Siemens Sequoia systems (Germany) equipped with a C3–7 probe in both Mengchao Hepatobiliary Hospital and Fujian Provincial Cancer Hospital. All sonographers underwent unified training before study initiation to ensure inter-center consistency. For each examination, the probe was applied with minimal contact pressure (< 10 kPa, approximately 0.5–1 N), sufficient only to maintain stable acoustic coupling without compressing the underlying tissue, in accordance with WFUMB elastography recommendations. The same acquisition mode (shear wave elastography, SWE) and manufacturer-recommended presets were used across centers.

In patients with multiple lesions, the largest lesion was selected for analysis. Recorded imaging parameters included satellite nodules, tumor diameter, capsule integrity, echogenicity, boundary definition, collateral circulation, and macrovascular invasion. Tumor and peritumoral stiffness were measured at 12 predefined sites: intra-tumoral regions (12, 3, 6, 9 o'clock positions and center; A–E), peri-tumoral regions (2, 5, 8, 11 o'clock; F1–F4), and distal liver parenchyma (1 cm, 2 cm from tumor margin and normal liver; G–I).(Figure 2)

At each site, five consecutive elasticity measurements were obtained during breath-holding, with the median value used to minimize motion artifacts. The change in tumor stiffness (ΔT) was defined as positive ($\Delta T > 0$) when ≥ 5 of 9 intra- and peri-tumoral points (A–F4) exhibited increased stiffness after six weeks of therapy, based on pilot observations showing that changes involving over half of the tumor–peritumor interface correlated best with treatment response. Similarly, $\Delta P > 0$ was defined when ≥ 2 of 3 distal points (G–I) increased. All measurements were performed under standardized acquisition conditions to minimize inter-operator variability.

Confirmed HCC

The diagnosis of hepatocellular carcinoma (HCC) can be confirmed through two primary methodologies. The first approach relies on imaging modalities, specifically the employment of contrast-enhanced ultrasound (CEUS), enhanced computed tomography (CT), or magnetic resonance imaging (MRI), which are evaluated based on the characteristic enhancement pattern typical of liver cancer, notably the rapid wash-in and wash-out of contrast agent. The second method involves obtaining a tissue sample directly from the tumor through a biopsy procedure. This dual-pathway approach allows for a comprehensive evaluation and confirmation of HCC.

Survival analysis

To further assess the clinical relevance of the TIPM model, overall survival (OS) was analyzed as a secondary endpoint. OS was defined as the time from treatment initiation to death from any cause or last follow-up. Patients who were alive at the time of analysis were censored at their most recent follow-up.Patients were stratified into high- and low-TIPM score groups according to the optimal cutoff value determined by receiver operating characteristic (ROC) analysis. Kaplan–Meier survival curves were generated to compare OS between the two groups, and differences were assessed using the log-rank test. Hazard ratios (HRs) and corresponding 95% confidence intervals (Cis) were calculated using univariate and multivariate Cox proportional hazards regression models to evaluate whether the TIPM score served as an independent prognostic factor.

Statistics

In this study, continuous variables are expressed as the mean ± standard deviation, while categorical variables are presented as frequencies and percentages. For continuous data following a normal distribution and homogeneity of variance, comparisons between groups were performed using the independent-samples *t* test; otherwise, the

Mann–Whitney *U* test was applied. Categorical variables were compared using the chi-square test.Variables that reached statistical significance in univariate analysis were incorporated into a multivariate binary logistic regression model, with a stepwise backward selection approach used to identify independent predictors. The relative importance of these predictors was further ranked using a random forest algorithm.Subsequently, the identified variables were categorized into ultrasound indicators, serological indicators, and combined indicators. Individual predictive models were constructed for each category, and a fusion model (Target Immunotherapy Predictive Model, TIPM) was developed by integrating the selected significant variables to improve predictive accuracy. The performance of the fusion model was compared with established clinical indices, including ALBI and AFP, across the training, internal validation, and external validation cohorts.Model performance was evaluated using receiver operating characteristic (ROC) curves and the area under the curve (AUC), with DeLong's test applied to assess statistical differences between AUCs. Calibration curves were generated, and both the Hosmer–Lemeshow (H–L) goodness-of-fit test and Brier score were used to evaluate model calibration and predictive reliability. Decision curve analysis (DCA) was further conducted to assess the net clinical benefit of each model.Finally, individualized risk scores were calculated for each patient based on the TIPM, and the optimal cutoff value was determined using the Youden index to derive sensitivity, specificity, accuracy, precision, and F1-score. All statistical analyses and visualizations were conducted using R statistical software (version 4.1.1), and a two-tailed P value < 0.05 was considered statistically significant.

Data availability

The datasets generated and/or analyzed during the current study are not publicly available due to being generated based on information collected during clinical care but are available in de-identified from the corresponding author on reasonable request at the study's close.

Received: 21 March 2024; Accepted: 6 November 2025
Published online: 22 December 2025

References

1. Llovet, J. M. et al. Hepatocellular carcinoma[J]. *Nat. Reviews Disease Primers*. **7** (1), 12–39. https://doi.org/10.1038/s41572-020-00240-3 (2021).
2. Sung, H. et al. Global cancer statistics 2020: GLOBOCAN estimates of incidence and mortality worldwide for 36 cancers in 185 Countries. *CA Cancer J. Clin.* **71** (3), 209–249. https://doi.org/10.3322/caac.21660 (2021).
3. Petrowsky, H. et al. Modern therapeutic approaches for the treatment of malignant liver tumours. *Nat. Reviews Gastroenterol. Hepatol.* **17** (12), 755–772. https://doi.org/10.1038/s41575-020-0314-8 (2020).
4. Yang, C. et al. Evolving therapeutic landscape of advanced hepatocellular carcinoma. *Nat. Reviews Gastroenterol. Hepatol.* **20** (4), 203–222. https://doi.org/10.1038/s41575-022-00704-9 (2023).
5. Llovet, J. M. et al. Immunotherapies for hepatocellular carcinoma. *Nat. Reviews Clin. Oncol.* **19** (3), 151–172. https://doi.org/10.1038/s41571-021-00573-2 (2022).
6. Yang, T-K. et al. Efficacy and safety of combined targeted therapy and immunotherapy versus targeted monotherapy in unresectable hepatocellular carcinoma: a systematic review and meta-analysis. *BMC Cancer*. **22** (1), 1085. https://doi.org/10.1186/s12885-022-10174-6 (2022).
7. Parra, N. S. et al. Advancements in the diagnosis of hepatocellular Carcinoma. *Int. J. Translational Med.* **3** (1), 51–65. https://doi.org/10.3390/ijtm3010005 (2023).
8. Illimoottil, M. & Ginat, D. Recent advances in deep learning and medical imaging for head and neck cancer treatment: MRI, CT, and PET Scans. *Cancers* **15** (13), 65–78. https://doi.org/10.3390/cancers15133267 (2023).
9. Jin, C. et al. Predicting treatment response from longitudinal images using multi-task deep learning. *Nat. Commun.* **12** (1), 1851–1862. https://doi.org/10.1038/s41467-021-22188-y (2021).
10. RMS, S. & AE, J. L. Ultrasound elastography: review of techniques and clinical Applications. *Theranostics* **7** (5), 1303–1329. https://doi.org/10.7150/thno.18650 (2017).
11. Zheng, T. et al. Noninvasive diagnosis of liver cirrhosis: qualitative and quantitative imaging biomarkers. *Abdom. Radiol.* **2** (11), 325–338. https://doi.org/10.1007/s00261-024-04225-8 (2024).
12. Haas, Y., Dosch, M. P. & Vogl, T. J. Response comparison of PLC and SLC with magnetic resonance elastography after TACE. *Sci. Rep.* **12** (1), 8317–8326. https://doi.org/10.1038/s41598-022-12478-w (2022).
13. Hou, S. et al. The course and prognostic value of tumor stiffness detected by ultrasound elastography for transarterial chemoembolization of hepatocellular carcinoma. *Quant. Imaging Med. Surg.* **13** (6), 3962–3972. https://doi.org/10.21037/qims-22-292 (2023).
14. Colloca, G. A. & Venturino, A. Radiographic and serologic response in patients with unresectable hepatocellular carcinoma receiving systemic antineoplastic treatments: A trial-level analysis. *Cancer* **12** (2), 1–11. https://doi.org/10.1002/cncr.35199 (2024).
15. Valero, C. et al. Pretreatment neutrophil-to-lymphocyte ratio and mutational burden as biomarkers of tumor response to immune checkpoint inhibitors. *Nat. Commun.* **12** (1), 729–745. https://doi.org/10.1038/s41467-021-20935-9 (2021).
16. Berlanga, A. et al. Neutrophil to lymphocyte ratio and cancer prognosis: an umbrella review of systematic reviews and meta-analyses of observational studies. *BMC Med.* **18** (5), 360–375. https://doi.org/10.1186/s12916-020-01817-1 (2020).
17. Chen, Y., Qi, Y. & Wang, K. Neoadjuvant chemotherapy for breast cancer: an evaluation of its efficacy and research progress. *Front. Oncol.* **13** (8), 1169010–1169025. https://doi.org/10.3389/fonc.2023.1169010 (2023).
18. Dall'Olio, F. G. et al. Tumour burden and efficacy of immune-checkpoint inhibitors. *Nat. Reviews Clin. Oncol.* **19** (2), 75–90. https://doi.org/10.1038/s41571-021-00564-3 (2022).
19. Kong, X. et al. Advances in imaging in evaluating the efficacy of neoadjuvant chemotherapy for breast cancer. *Front. Oncol.* **12** (11), 816297–816316. https://doi.org/10.3389/fonc.2022.816297 (2022).
20. Chen, J. et al. Apparent diffusion coefficient and tissue stiffness are associated with different tumor microenvironment features of hepatocellular carcinoma. *Eur. Radiol.* **34** (11), 6980–6991. https://doi.org/10.1007/s00330-024-10743-2 (2024).
21. Wang, Y. et al. Reduced tumor stiffness quantified by tomoelastography as a predicative marker for glypican-3-positive hepatocellular carcinoma. *Front. Oncol.* **12**, 962272. https://doi.org/10.3389/fonc.2022.962272 (2022).
22. Yoo, S-K. et al. Pre-treatment serum albumin and mutational burden as biomarkers of response to immune checkpoint blockade. *NPJ Precision Oncol.* **6** (1), 23–27. https://doi.org/10.1038/s41698-022-00267-7 (2022).
23. Zheng, M. Serum albumin: a Pharmacokinetic marker for optimizing treatment outcome of immune checkpoint blockade. *J. Immunother. Cancer*. **10** (12), 12–21. https://doi.org/10.1136/jitc-2022-005670 (2022).

24. Stares, M. et al. Hypoalbuminaemia as a prognostic biomarker of first-line treatment resistance in metastatic non-small cell lung cancer. *Front. Nutr.* **8** (12), 734735–734743. https://doi.org/10.3389/fnut.2021.734735 (2021).
25. Cottrell, T. R. et al. Society for immunotherapy of cancer (SITC) consensus statement on essential biomarkers for immunotherapy clinical protocols. *J. Immunother. Cancer*. **13** (3). https://doi.org/10.1136/jitc-2024-010928 (2025).
26. Sadagopan, N. & He, A. R. Recent progress in systemic therapy for advanced hepatocellular Carcinoma. *Int. J. Mol. Sci.* **25** (2), 1259–1274. https://doi.org/10.3390/ijms25021259 (2024).
27. Jeng, L-B., Wang, J. & Teng, C-F. Predictive biomarkers of immune checkpoint Inhibitor-Based Mono- and combination therapies for hepatocellular Carcinoma. *J. Cancer*. **15** (2), 484–493. https://doi.org/10.7150/jca.90128 (2024).
28. Tu, H. et al. Revolutionising hepatocellular carcinoma surveillance: Harnessing Contrast-enhanced ultrasound and serological indicators for postoperative early recurrence Prediction. *Med. (Baltim).* **11** (21), 1265–1278DOI (2023).
29. Zhou, H. et al. Prognostic factors and predictive nomogram models for early death in elderly patients with hepatocellular carcinoma: a population-based study. *Front. Mol. Biosci.* **10** (7), 16–29. https://doi.org/10.3389/fmolb.2023.1275791 (2023).
30. Piao, M. et al. Conversion surgery after immune checkpoint Inhibitor-Based combination therapy for initially unresectable hepatocellular carcinoma: A retrospective cohort Study. *Liver Cancer*. **14** (4), 456–473. https://doi.org/10.1159/000543994 (2025).

Acknowledgements

We are grateful to Yuzhen Gao for selflessly providing professional advice on the statistical aspects of this paper and for conducting a thorough review.

Author contributions

Haibin Tu concept and write this paper. Siyi Feng made data statistical, Lihong Chen, Yujie Huang, Juzhen Zhang, Suyu Peng, Dingluan Lin make follow-up, Xiaojian Ye correct and give guide for this paper.

Funding

This work was supported by the Institutional Research Project of Mengchao Hepatobiliary Hospital of Fujian Medical University (Grant No. 2025-LCYJ-05), Fujian Natural Science Foundation (NO.2023J011480), Natural Science Foundation of Fujian Province, China (Grant NO:2022J011285), Fuzhou Municipal Bureau of Science and Technology Program Fund (2021-S-109), Provincial subsidy fund for health and wellness from Fujian Provincial Department of Finance (Grant NO: BPB-2022YXJ) and Fujian Provincial Health Technology Project (Grant NO:2020GGB032).

Declarations

Competing interests

The authors declare no competing interests.

Ethics approval

This study was reviewed and approved by Mengchao Hepatobiliary Hospital Ethics Committee (NO. 2021_084_01). All the experiments in this study were conducted in accordance to the relevant guidelines and regulations in accordance to the Declaration of Helsinki.

Consent to participate

Owing to its retrospective design, the necessity for obtaining informed consent was exempted. Additionally, we confirm that all methods were performed in accordance with relevant guidelines and regulations declared in Investigative Radiology.

Additional information

Correspondence and requests for materials should be addressed to X.Y.